

Magma mixing and convective compositional layering within the Vesuvius magma chamber

Lucia Civetta¹, Rita Galati¹, and Roberto Santacroce²

¹ Dipartimento di Geofisica e Vulcanologia, Largo San Marcellino 10, Università di Napoli, I-80138 Napoli, Italy

² Dipartimento di Scienze della Terra, via Santa Maria 53, Università di Pisa, I-56100, Italy and Istituto Internazionale di Vulcanologia, CNR, P.zza Roma 2, I-95129 Catania, Italy

Received June 20, 1989/Accepted December 12, 1990

Abstract. The pumice-fall deposits of the last two Plinian eruptions of Vesuvius – A.D. 79 “Pompei” and 3700 B.P. “Avellino” – show a marked vertical compositional variation from white phonolite at the base to grey tephritic phonolite at the top. In both Avellino and Pompei sequences a compositional gap separates white from grey pumice. Grey and white pumice have distinct Sr and Nd isotopic compositions (grey pumice: $^{87}\text{Sr}/^{86}\text{Sr}=0.70749\text{--}56$, $^{143}\text{Nd}/^{144}\text{Nd}=0.512507$ for Pompei; 0.70760–69, 0.512504 for Avellino; white pumice: 0.70757–78 for Pompei; 0.70729–42 for Avellino). K-feldspar separated from both grey and white pumice has, in all cases, a “white” $^{87}\text{Sr}/^{86}\text{Sr}$ ratio (0.70766–79 for Pompei, 0.70728–33 for Avellino). The observed variations are interpreted as reflecting a pre-eruptive zonation of the magma chamber. Although mineralogical evidence of interaction between magma and calcareous country rocks exists in both eruptions, crustal contamination has not significantly modified the isotopic signatures of the erupted products. Petrographic and isotopic evidence of syneruptive magma mingling occur in Pompei grey pumice as well as in Avellino white and grey pumice, but they do not fully explain all the observed geochemical and isotopic variations. These variations are related to the complex refilling history of the magmatic system and result by fractional crystallization and mixing processes acting within the magma chamber. Preliminary data from other Plinian and subplinian eruptions of the Somma-Vesuvius point out the repetitive behaviour of $^{87}\text{Sr}/^{86}\text{Sr}$ variation in the last 25 000 years, hence suggesting a single magma chamber and continuity of the feeding system.

Introduction

The origin of chemical zonation in shallow magma chambers is controversial. Different processes have been proposed, involving crystal-liquid fractionation, crustal contamination and magma mixing (e.g. Barberi

et al. 1978; Hildreth 1979, 1981; Wolff and Storey 1984; Fridrich and Mahood 1987; Bacon and Drittt 1988). In this regard, radiogenic isotopes may provide an important contribution. They are petrogenetic markers not affected by chemical fractionation associated with crystallization and can allow discrimination between closed- and open-system behaviour of a magma chamber (e.g. Verma 1983; Wörner et al. 1985; Hildreth 1987; Mahood and Halliday 1988; Palacz and Wolff 1989).

This paper provides a detailed Sr and Nd isotopic study of the deposits of the two last Plinian eruptions of Vesuvius (“Pompei”, A.D. 79 and “Avellino”, 3700 B.P.), both displaying a marked vertical compositional variation from white phonolite to grey tephritic phonolite (Lirer et al. 1973; Barberi et al. 1981; Sheridan et al. 1981; Cornell and Sigurdsson 1984, 1987; Wolff and Storey 1984; Sigurdsson et al. 1985, 1987, 1990; Joron et al. 1987; Santacroce (ed.) 1987). The origin of this chemical zonation is still debated. Major and trace element distribution is consistent with an origin mainly due to crystal fractionation within a closed magma chamber (Barberi et al. 1981; Wolff and Storey 1984). However evidence for magma mixing (Joron et al. 1987; Cornell and Sigurdsson 1987; Sigurdsson et al. 1990) and minor wall-rock contamination (Barberi et al. 1981), also exists.

The juvenile component of both Avellino and Pompei deposits exhibits widely variable $^{87}\text{Sr}/^{86}\text{Sr}$ and $^{143}\text{Nd}/^{144}\text{Nd}$ ratios. From the more evolved to the less evolved products, the $^{87}\text{Sr}/^{86}\text{Sr}$ ratio shows either a general increase (Avellino) or decrease (Pompei) in value. The corresponding trends of the $^{143}\text{Nd}/^{144}\text{Nd}$ ratio are the reverse of those for the $^{87}\text{Sr}/^{86}\text{Sr}$.

Evidence for a mainly magmatic origin of the isotopic variations will be presented and discussed. Comparison with the isotopic data of other Vesuvius products (Cortini and Hermes 1981; Civetta et al. 1987; Galati R. unpublished data), allows us to define a general picture of the isotopic history of the volcano in the last 25 000 years, which suggests a repetitive open-system behaviour of the Vesuvius magma chamber.

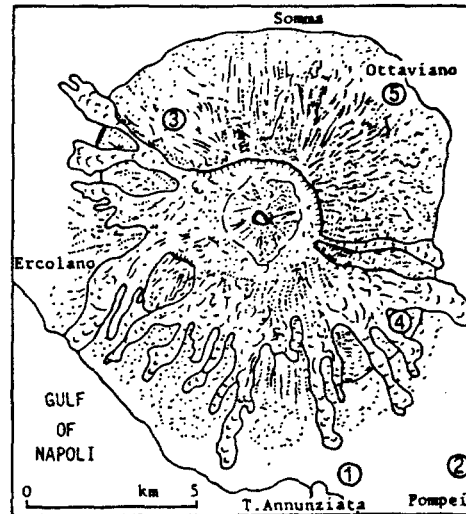
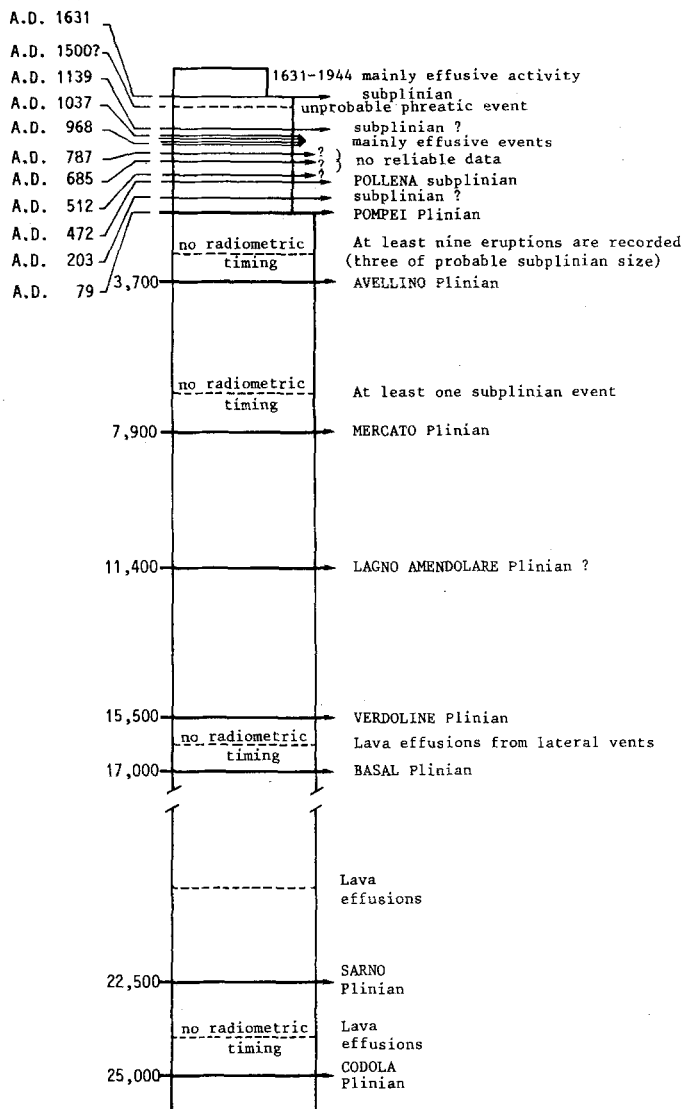


Fig. 1. General sequence of events during the last 25 000 years of Somma-Vesuvius activity (modified after Arnò et al. 1987). Location of the sampling sites in the inset: 1, Oplontis (Torre Annunziata) excavations; 2, Pompeii excavations; 3, Lagno di Pollena quarries; 4, Pozzelle quarry; 5, Trapolino quarry

Volcanic history and types of activity of Somma-Vesuvius

Somma-Vesuvius is a composite central volcano (1281 m a.s.l.), consisting of an older, repeatedly collapsed strato-volcano (Monte Somma caldera) and a more recent cone, Vesuvius, built inside the caldera.

The eruptive history of Somma-Vesuvius in the last 25 000 years is summarized in Fig. 1 (Arnò et al. 1987). The caldera collapse has been correlated with the eruption of the "Basal Pumice", (17 000 B.P., Delibrias et al. 1979); since that time the shape and the size of the caldera have modified several times following the rapid discharge of large volumes of magma, mainly during Plinian eruptions.

Three main categories of eruptions have been distinguished (Santacroce 1983): small volume (ca. 0.01 km^3) explosive and effusive; medium volume (ca. 0.1 km^3) subplinian; and large volume ($>1 \text{ km}^3$) Plinian. The eruptions of the first type characterize the most recent activity (1637–1944) and close short cycles of strombolian activity, reflecting open chimney conditions. Me-

dium- and large-size events occurred after a long quiescence period. The most common feature of these eruptions is an initial Plinian fall phase, interrupted briefly by partial column collapses and followed by the emplacement of surges, pyroclastic flows, mud hurricanes and lahars (Sheridan et al. 1981; Sigurdsson et al. 1985). Interaction between magma and phreatic water usually occurs during the final stages of these eruptions (Sheridan et al. 1981; Barberi et al. 1989, 1990).

Three "magmatic" periods have been recognized in the last 25 000 years: (1) the oldest one (25 000 to 11 400 B.P.) was characterized by slightly undersaturated lavas (K-basalt to K-latitude) and tephra (K-latitude to K-trachyte). Activity was dominated by five Plinian eruptions; (2) during the second period (7900 B.P. to A.D. 79), three Plinian eruptions occurred, alternating with long periods of repose and minor explosive events: composition ranges from tephritic phonolite to phonolite; and (3) the last period of activity includes at least two subplinian eruptions, several other explosive and effusive events, and a long interval (1631–1944) of strombolian activity, frequently interrupted by severe

(1906-type) effusive and explosive eruptions; composition ranges from tephritic leucitite to leucititic phonolite.

Analytical procedure

Macroscopically homogeneous composite pumice samples from Avellino and Pompei sequences were pulverized in an agate mortar and washed in quartz-distilled water for 50 h. Minerals were separated using a Franz magnetic separator and heavy liquids and then by hand picking under a microscope. Major and trace elements were measured by XRF except MgO (AAS). Isotopic determinations were made using a VG-350 double-collector mass-spectrometer. Sr was separated by a conventional ion-exchange technique and analysed on single Ta filament. Analysis of NBS 987 standard yielded an average $^{87}\text{Sr}/^{86}\text{Sr}$ ratio of 0.710264 ± 5 (2σ). Typical total blank was less than 4 ng. The $^{87}\text{Sr}/^{86}\text{Sr}$ ratio was not age-corrected, as the correction was below the level of significance. Nd was separated by inverse-phase chromatography and analysed as metal on one Ta side-filament, of a triple-filament assembly. Analysis of BCR-1 standard yielded a value of $0.51265 \pm 1.2\sigma_m$; errors on $^{87}\text{Sr}/^{86}\text{Sr}$ and $^{143}\text{Nd}/^{144}\text{Nd}$ refer to the last digit.

The A.D. 79 eruption

Recent studies provide a detailed reconstruction of the eruption (Sheridan et al. 1981; Sigurdsson et al. 1982, 1985, 1990; Carey and Sigurdsson 1987; Barberi et al. 1989). The studied samples were collected at three sites – the Oplontis excavations, and the Pozzelle and Pollena quarries – and cover the entire depositional sequence (Fig. 2). Following Barberi et al. (1989) four main phases have been recognized.

1. Phreato-magmatic explosive opening

This phase (layer “A” of Sigurdsson et al. 1985) is represented by two samples (84.25 and 87.26) collected at the Pozzelle quarry (Fig. 2). The analysed pumices were separated by a coarse ash-fall deposit containing abundant accretionary lapilli. The juvenile fraction represents about 22% of the deposit (Barberi et al. 1989). The erupted mass is negligible.

2. Plinian *s. s.* phase

Both fallout and flow deposits are ascribed to this phase of the eruption, (whose duration is of 19 h according to Carey and Sigurdsson 1987). The fall deposit (Oplontis and Pozzelle) shows a sharp upward transition from white phonolitic to grey tephritic phonolitic pumice. The deposition was continuous during the white-pumice fallout. In areas within 6–7 km from the vent the deposition of the grey-pumice fallout was interrupted at least four times by the emplacement of pyroclastic flows and associated ash-cloud surges. The de-

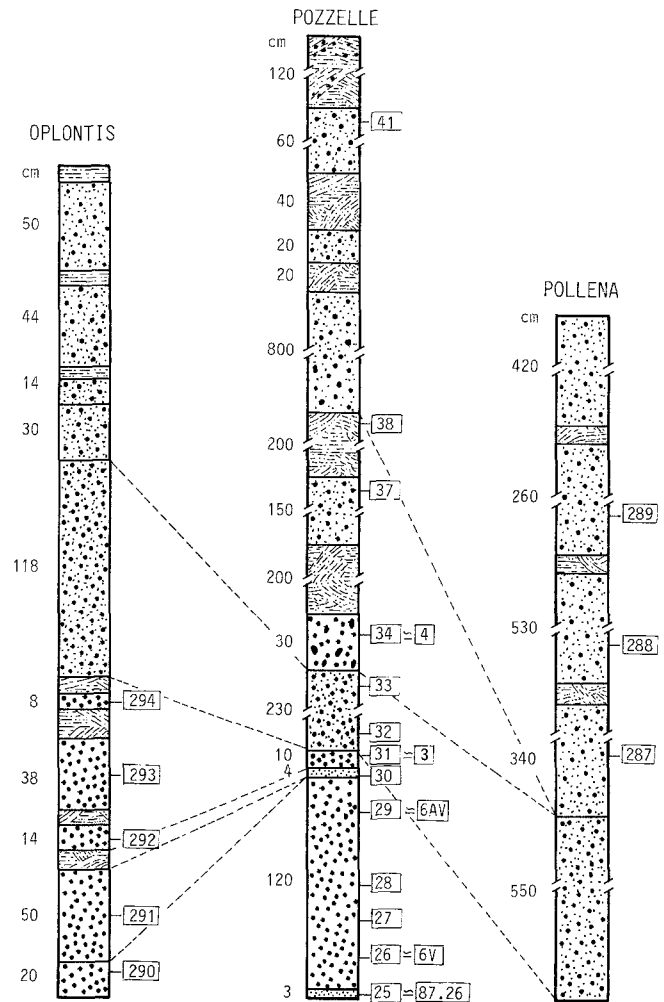


Fig. 2. Suggested correlation between the stratigraphic sections of Pompei eruption deposits discussed in the text. Location of sections in Fig. 1. Thickness (cm) on the left of each column. Sample numbers on the right. Samples 84.25, 84.26, 87.27, 87.28, 84.29, 84.30, 84.32, 87.34, 87.37, 87.38, 87.41 are reported in Fig. 2 omitting 87 and 84, which refer to the year of collection

posits of this phase are largely incomplete at Pozzelle, where most of the grey pumice is not present. Pumice for analysis was separated from samples 290 (hand split into white, [A], and grey [B] pumice), 291, 292, 293, 294 (Oplontis grey fall deposit), 84.26, 6V 87.27, 87.28, 84.29, 6AV (Pozzelle white fall), 84.30 (Pozzelle ash-cloud surge), 87.31, 3 (Pozzelle grey fall), 84.32, 84.33 and 87.33 (Pozzelle pumice flow) (Fig. 2). Erupted masses are approximately 2×10^9 tons and 5.5×10^9 tons for white and grey pumice respectively (Macedonio et al. 1989, after the volume estimate of Sigurdsson et al. 1985).

3. Dry surge and flow phase

After the collapse of the Plinian column, the activity was interrupted briefly by slumping of the conduit walls and moderate obstruction of the vent. Barberi et al. (1989) suggest that the tuff breccia layer (sample n.

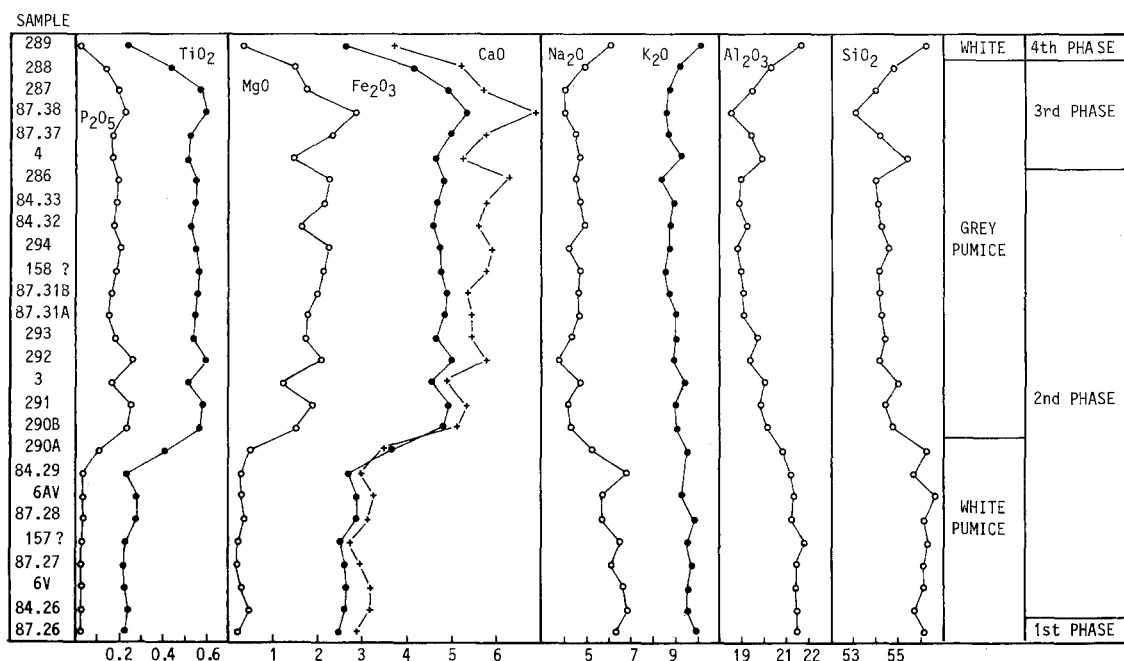


Fig. 3. Vertical chemical variations in an idealized section of the A.D. 79 Pompei eruption. All water-free and recalculated to 100%. Sample locations and numbers as in Fig. 2. Sample 87.26 is equivalent to 84.25 ("25" in Fig. 2); samples 290A and 290B, as well as

87.31A and 87.31B were obtained by hand splitting of heterogeneous pumice samples ("290" and "31" in Fig. 3). Samples 157 and 158 have been collected at Pompei excavations and have an uncertain stratigraphic position in the proposed ideal section

34 in Fig. 2) is the result of the explosive clearing of the chimney (morning of 25 August). The third phase possibly lasted until the late morning or early afternoon of 25 August. The deposits of this phase (as well as those of the next one) have a low content of juvenile fragments (less than 30%, Barberi et al. 1989). Pumice was separated from samples 87.34, 87.37, 87.38 (Pozzelle quarry) and 287, 288 (Pollena quarry). Erupted material is about $0.5\text{--}0.6 \times 10^9$ tons.

4. Wet surges and flows phase

During this phase, of unknown (days?, months?) duration, all eruptive phenomena were progressively decreasing. A peculiar aspect is the "wet" nature of the deposits (occurrence of accretionary lapilli, vesiculated tuff beds and soft sediment deformation). Pumice was separated from samples 87.41 [Pozzelle, hand split in white (c) and dark (s) pumice] and 289 (Pollena) (Fig. 2). Less than 0.5×10^9 tons of material was ejected. Samples 157 and 158 are from white and grey Plinian fall deposits at Bottaro, near Pompei (Barberi et al. 1981).

Chemical and mineralogical data on the products of the Pompei eruption (including some of the samples studied in this paper) are in Barberi et al. (1981) and in Joron et al. (1987). A new set of chemical analyses is reported in Table 1. As previously noticed, the Plinian s.s. deposits exhibit a compositional variation from white phonolite at the base of the sequence to grey tephritic phonolite at the top and an upward increase in mafic phenocrysts (Table 2). Pumice collected from the 3rd and 4th phase deposits define a compositional trend

reversing that of the Plinian phase (Fig. 3). A decrease of the magma discharge rate, also notified by Cornell and Sigurdsson (1987), Sigurdsson et al. (1987) and Sigurdsson et al. (1990), was probably responsible for the tapping of roofward magma "trapped" in the chamber (Spera et al. 1986).

The main phenocryst phases are clinopyroxene, biotite, sanidine and leucite. Later in the crystallization sequence other minerals formed (ferripargasitic amphibole, Fe-Ti oxides, plagioclase, scapolite, cancrinite and garnet), probably also as a result of interaction between magma and limestone (high CO_2 pressure). Rare olivine and anorthite-bytownite plagioclase also occur. Magma mixing as well as crystal fractionation processes within the chamber are suggested by the oscillatory compositional zoning of clinopyroxene and garnet, mainly in the grey-pumice (Barberi et al. 1981; Joron et al. 1987). Indications of sineruptive mingling arise from the K-rich sanidine microlites of the grey pumice, that are richer in K than the sanidine phenocrysts and from "occasional wetting of the crystals by their former host melts" (Cornell and Sigurdsson 1987).

The 3700 B.P. Avellino eruption

The pumice-fall deposits of this eruption are similar to those of the Pompei eruption. Both show an abrupt change in pumice colour from white to grey roughly midway through the deposit and both contain similar xenolithic ejecta. Their different areal distributions prevent confusion in identifying the deposits (Lirer et al. 1973), but other discriminants are: different lithic to

Table 1. Chemical analyses (major %, trace ppm) of composite pumice samples from Pompei eruption deposits

Sample	87.26	84.26	6V	87.27	157	87.28	6AV	84.29	290A	290B	291	3	292	293	87.31A
SiO ₂	56.25	55.60	55.90	56.05	56.23	56.10	56.32	55.65	55.95	54.66	54.22	54.92	53.90	54.35	54.20
TiO ₂	0.22	0.24	0.23	0.22	0.23	0.28	0.28	0.25	0.39	0.57	0.59	0.51	0.59	0.54	0.57
Al ₂ O ₃	21.50	21.40	21.40	21.50	21.80	21.19	21.60	21.50	20.70	19.80	19.40	20.00	19.40	19.70	19.10
Fe ₂ O ₃	2.50	2.60	2.60	2.60	2.60	2.90	2.90	2.70	3.60	4.60	5.00	4.20	5.00	4.60	4.90
MnO	0.13	0.13	0.14	0.13	0.13	0.14	0.14	0.14	0.13	0.14	0.14	0.14	0.15	0.13	0.15
MgO	0.18	0.40	0.31	0.18	0.19	0.35	0.32	0.32	0.39	1.61	1.93	1.26	2.10	1.76	1.82
CaO	2.90	3.20	3.20	2.90	2.70	3.10	3.30	3.00	3.90	5.20	5.50	4.70	5.90	5.40	5.50
Na ₂ O	6.30	6.80	6.60	6.30	6.50	6.00	5.80	6.80	5.14	4.22	4.10	4.90	3.80	4.30	4.60
K ₂ O	10.00	9.60	9.60	10.10	9.60	9.90	9.60	9.60	9.60	9.00	8.90	9.20	8.90	9.00	9.00
P ₂ O ₅	0.02	0.02	0.02	0.02	0.02	0.04	0.04	0.04	0.10	0.20	0.22	0.17	0.25	0.19	0.17
l.o.i.	3.43	4.08	3.21	3.18	2.65	3.09	2.36	4.26	2.84	2.09	2.15	3.01	2.33	2.63	2.45
Nb	70	70	67	66	68	65	61		68	50	45				51
Zr	357	357	351	343	340	333	334		309	301	258	272			259
Sr	347	347	279	370	350	464	415		610	810	908	896			912
Rb	397	397	385	399	393	385	408		362	346	356	346			354
Ba	112			120	190	248			610	1120					955
La	89			88	89	87			80	70					72
Ce	158			161	156	145			150	134					146

Sample	87.31B	158	294	84.32	84.33	87.33	286	4	87.37	87.38	287	288	289
SiO ₂	54.19	54.03	54.20	54.17	53.98	54.20	54.10	54.96	53.90	52.84	54.00	54.42	56.00
TiO ₂	0.57	0.57	0.55	0.53	0.55	0.54	0.56	0.51	0.54	0.60	0.57	0.44	0.25
Al ₂ O ₃	19.20	19.30	19.00	19.40	19.10	19.50	19.10	19.80	19.30	18.50	19.50	20.10	21.60
Fe ₂ O ₃	5.00	4.80	4.80	4.60	4.70	4.50	4.80	4.30	4.90	5.20	4.80	4.00	2.60
MnO	0.15	0.12	0.13	0.14	0.14	0.14	0.14	0.14	0.15	0.15	0.14	0.14	0.14
MgO	2.00	2.17	2.21	1.68	1.94	1.54	2.12	1.32	2.12	2.87	1.81	1.46	0.39
CaO	5.40	5.80	6.00	5.60	5.70	5.30	6.00	4.80	5.50	6.90	5.70	5.10	3.40
Na ₂ O	4.50	4.50	4.30	4.90	4.80	4.90	4.40	4.70	4.60	4.40	4.40	5.10	5.70
K ₂ O	8.90	8.50	8.60	8.80	8.90	9.20	8.60	9.30	8.80	8.30	8.90	9.10	9.90
P ₂ O ₅	0.19	0.21	0.20	0.18	0.19	0.17	0.20	0.17	0.20	0.24	0.19	0.14	0.04
l.o.i.	2.46	2.44	2.70	2.62	3.14	2.38	2.92	3.01	2.42	2.87	2.69	3.13	4.01
Nb	51	50	50					45	52	49	50	54	86
Zr	254	255	267					250	267	251	265	295	388
Sr	888	730	750					805	819	886	970	731	386
Rb	356	334	342					360	354	348	344	374	415
Ba	950	920	970						838	931	1080		
La	70	77	71						74	71	72		
Ce	143	130	130						149	141	133		

Major and trace element determined by XRF, with the exception of MgO by AA. FeO + Fe₂O₃ as Fe₂O₃. Major element analyses are water-free and recalculated to 100%

Table 2. Modal estimates of phenocrysts content (point counting) in Pompei and Avellino pumice

Phase	Pompei						Avellino			
	White pumice			Grey pumice			White pumice		Grey pumice	
	157	6V	6AV	3	158	4	118	5BV	5V	116
K-feldspar	2.8±0.7	3.5±0.8	2.9±0.7	1.1±0.4	0.3±0.2	0.9±0.4	7.4±1.0	9.3±1.2	14.5±1.4	12.7±1.3
Clinopyroxene	1.3±0.4	2.1±0.6	2.8±0.7	5.3±0.9	4.3±1.0	4.9±0.9	7.1±1.0	8.5±1.1	1.2±0.4	0.6±0.3
Biotite	0.4±0.3	0.2±0.2	0.5±0.3	3.0±0.7	2.4±0.6	3.2±0.7	1.2±1.0	2.1±0.6	0.7±0.3	0.3±0.2
Leucite	Trace	0.3±0.2	0.4±0.3	0.2±0.2	0.2±0.2	0.7±0.3	Absent	Absent	Absent	Absent
Nepheline	Absent	Absent	Absent	Absent	Absent	Absent	Trace	Trace	0.5±0.3	Trace
Amphibole	Trace	Trace	Trace	Trace	Trace	0.1±0.1	0.1±0.1	0.3±0.2	0.4±0.3	0.5±0.3
Fe-Ti oxides	0.6±0.3	0.1±0.1	Trace	0.3±0.2	0.7±0.3	Trace	0.4±0.3	0.4±0.3	Trace	0.4±0.3
Garnet	Trace	0.2±0.2	Trace	0.2±0.2	Trace	Trace	0.2±0.2	0.7±0.3	0.2±0.2	Trace
Scapolite	Trace	Absent	Trace	Trace	Trace	Trace	0.9±0.4	Trace	Trace	0.3±0.2
Other	Trace	Trace	0.2±0.2	0.1±0.1	Trace	Trace	0.6±0.3	0.2±0.2	0.6±0.3	0.4±0.2
Groundmass + vesicles	94.9	93.5	93.2	89.8	92.1	90.2	82.1	78.5	81.9	84.8

Table 3. Chemical analyses (major wt%, trace ppm) of composite pumice samples from Avellino eruption deposits at Trapolino quarry

White pumice						Grey pumice						w	g
Sample	AV1	5V	AV2	AV3	AV4	AV5c	AV5i	AV5s	5BV	AV6	AV7	116	118
SiO ₂	57.20	56.80	57.00	57.50	56.50	55.50	55.00	54.50	54.40	54.50	54.60	57.30	54.00
TiO ₂	0.17	0.11	0.12	0.10	0.12	0.30	0.41	0.50	0.47	0.46	0.48	0.12	0.50
Al ₂ O ₃	22.20	22.60	22.20	22.40	22.00	20.80	20.40	19.60	19.80	19.70	19.60	22.40	19.30
Fe ₂ O ₃	1.90	1.80	1.70	1.70	1.80	3.30	4.10	4.70	4.70	4.80	4.60	1.90	4.60
MnO	0.13	0.12	0.13	0.13	0.13	0.13	0.14	0.15	0.14	0.14	0.14	0.10	0.11
MgO	0.22	0.12	0.12	0.06	0.16	1.00	1.37	1.89	2.36	2.64	2.94	0.20	2.61
CaO	2.10	1.90	1.90	1.40	2.80	4.00	4.80	5.50	5.60	6.00	6.00	1.90	6.60
Na ₂ O	8.80	9.40	9.40	9.50	9.30	7.50	6.40	5.80	5.40	5.60	5.40	8.90	5.30
K ₂ O	7.50	7.20	7.40	7.30	7.10	7.40	7.30	7.20	6.90	6.90	6.80	7.20	6.70
P ₂ O ₅	0.03	0.02	0.02	0.01	0.03	0.13	0.18	0.24	0.23	0.21	0.23	0.02	0.24
l.o.i.	3.08	3.00	3.42	3.03	3.11	3.35	2.54	2.76	2.08	1.83	2.01	2.65	2.41
Nb	146	155	162	159	157	109	90	65	73	78	69	146	64
Zr	772	892	856	843	837	592	486	402	437	426	403	678	339
Sr	209	123	172	136	170	335	486	608	479	551	535	171	488
Rb	528	539	570	564	554	453	400	369	367	368	365	529	329
Ba												214	886
La												66	71
Ce												118	120

Major and trace element determined by XRF with the exception of MgO by AA. Samples 116 w (white pumice) and 118 g (grey pumice) are from Traianello quarry (Fig. 1). $\text{FeO} + \text{Fe}_2\text{O}_3 = \text{Fe}_2\text{O}_3$. Major elements analysed are water-free and recalculated to 100%

pumice proportions, mineralogy and chemical composition. No detailed stratigraphic correlations have been made so far among Avellino deposits and no detailed reconstruction of events is available. Therefore no composite section of the Avellino deposits is provided. Samples were collected at Trapolino quarry, where a 110 cm thick fallout deposit occurs. As for Pompei, the last stages of the Plinian fallout were accompanied and followed by the emplacement of pyroclastic flows, pyroclastic surges and lahars. No data are presently available on pumice from these deposits.

The distinctly lower K/Na ratio of the Avellino pumice in respect to the Pompei one is reflected by the different feldspathoid, which is nepheline in the Avellino pumice, but leucite in the A.D. 79 pumice. Other phenocrysts are, as in Pompei: clinopyroxene, biotite and sanidine (K-poorer than in Pompei, Barberi et al. 1981). Avellino pumice is more porphyritic than Pompei pumice and the phenocryst content increases from white to grey pumice.

The chemical variations observed in the Avellino pumice-fall deposit at Trapolino quarry (Table 3 and Fig. 4) are similar to the pattern of the Pompei 2nd phase (Fig. 3), although the Avellino compositional range extends to more evolved compositions. This possibly reflects the longer repose period of Vesuvius before the Avellino eruption (Santacroce 1983).

The mineralogical markers of reaction between magma and calcareous country rocks (scapolite, cancrinite, garnet) are much more abundant than in Pompei pumice (Table 2), while the occurrence of magma mixing within the Avellino magma chamber is revealed by similar mineralogical characteristics. Abundant banded white-grey pumice in the lowermost grey fall bed reveals syneruptive mingling.

Geochemical data

The chemical and mineralogical variations of Pompei and Avellino pumices have been interpreted by Barberi et al. (1981) and Joron et al. (1987) in terms of liquid lines of descent toward the phonolitic minimum at 1–2 kb $P_{\text{H}_2\text{O}}$. The more differentiated composition of Avellino white pumice reflects its closer plot to the minimum, in agreement with its lower temperature (heating stage thermometry) reported by Barberi et al. (1981) (780–820°C for the crystallization of sanidine, scapolite and nepheline of Avellino white pumice; 850–870°C for the crystallization of sanidine of Pompei white pumice).

Calculations based on major elements composition and mineral chemistry suggest that the grey-white transitions are dominated by fractionation of sanidine, clinopyroxene and scapolite (or nepheline) in the Avellino sequence and of clinopyroxene and leucite in the Pompei sequence (Barberi et al. 1981). Trace element distribution is coherent with the results of the Avellino fractionation model, while the marked Sr depletion of Pompei white pumice would require significant feldspar fractionation, as suggested by Joron et al. (1987). In both cases the strong depletion in heavy REE of white pumice (Joron et al. 1987; Wolff and Storey 1984), with respect to the grey one, requires garnet fractionation (melanite is a common phase of both sequences), as emphasized for Pompei by Wolff and Storey (1984). According to these authors, the distribution of Pompei trace elements may be explained by fractionation of the observed phenocryst assemblage; they suggest that "sidewall crystallization and consequent boundary layer uprise to form a capping layer at the top of the system may be a plausible mechanism for the generation of the zonation".

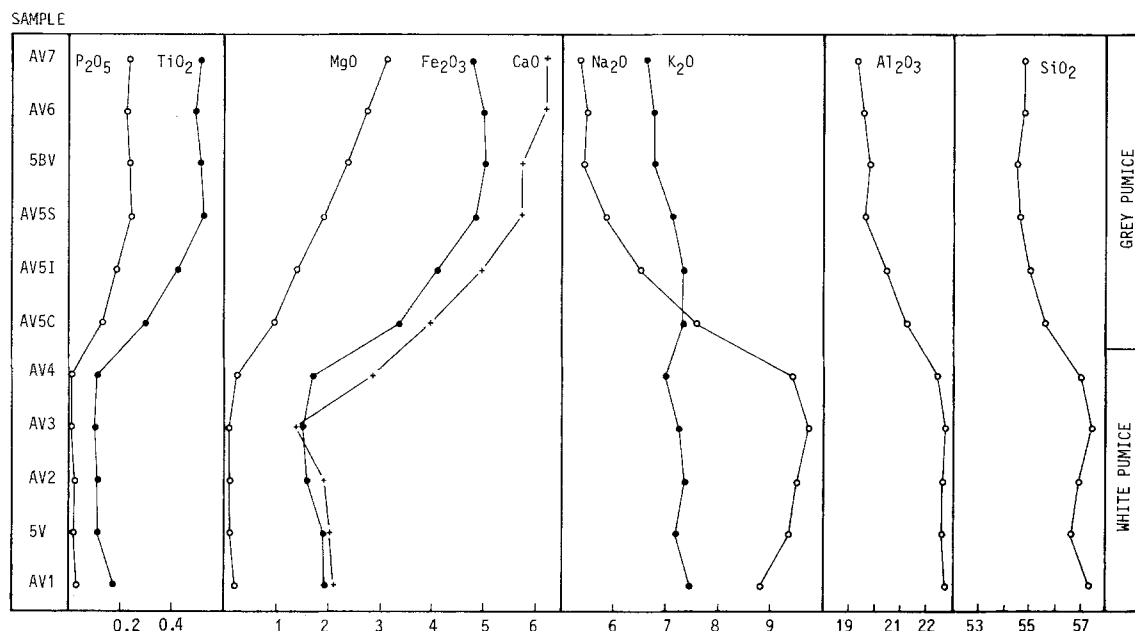


Fig. 4. Vertical chemical variations in the Avellino fallout deposit sampled at the Trapolino quarry (Fig. 1). Sampling was executed about every 20 cm AV1 to AV7. Sample AV5 (base of the grey pu-

mice) was hand split in three portions (c, i, s) according to slightly different pumice colours. $\text{FeO} + \text{Fe}_2\text{O}_3$ as Fe_2O_3 . Analyses are water-free and recalculated to 100%

Furthermore Avellino and Pompei pumices have different constant Zr/Nb ratio and different Sr vs Zr distribution (Fig. 5), indicative (in the case of fractional crystallization processes) of Pompei higher Sr bulk distribution coefficient. At the same degree of differentiation (similar MgO% content), Pompei pumice has higher concentrations of REE, Ba and Sr, with respect to the Avellino pumice, which in turn is more enriched in Zr, Nb and Rb.

The chemical zonation of the Pompei and Avellino pyroclastic deposits (Figs. 3 and 4) appears characterized by two-fold, stepwise gradients rather than by continuous variations. The white-grey transition is in fact a compositional gap, and internal compositional variations of both white and grey pumice are moderate by comparison. This may be interpreted as evidence of magmatic convection (Turner 1980; Hildreth 1981; Fridrich and Mahood 1987) within two contrasting layers, each roughly homogeneous in temperature, composition and density. A density gap between "white" and "grey" magmas has been suggested by Carey and Sigurdsson (1987), and DRE densities of 2.3 and 2.5 g/cm^3 are reported by Sigurdsson et al. (1987). A temperature gap could be also invoked on the base of the markedly higher melt homogenization temperature shown by melt inclusions in Avellino clinopyroxene (950–1050°C), with respect to salic phenocrysts (780–820°C; Barberi et al. 1981).

Isotopic results

The $^{87}\text{Sr}/^{86}\text{Sr}$ ratio (Table 4, Figs. 6 and 7), was measured on seven composite pumice samples from the Avellino fallout deposit and on 28 composite pumice

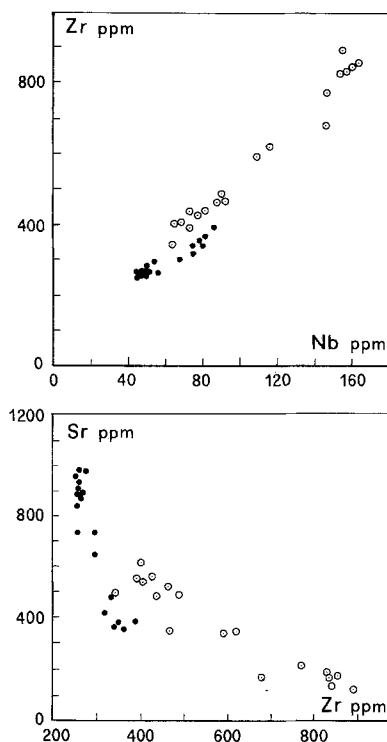


Fig. 5. Zr vs Nb and Sr vs Zr plots of Pompei and Avellino pumice. Pompei: full circle; Avellino: open circle

samples from the Pompei sequence. Three samples were hand split into two (84.41 and 87.31) or three (AV5) portions, according to variation in pumice colour. In all cases, results were the same within the analytical error. At Pozzelle quarry, samples were collected during two field surveys at five levels (25, 31, 33, 37, 38 in Fig. 2)

Table 4. $^{87}\text{Sr}/^{86}\text{Sr}$ ratios of pumice, K-feldspar, glass and carbonate xenoliths

Sample	Location	Whole-rock	$^{87}\text{Sr}/^{86}\text{Sr}$ K-feldspar	Glass
Avellino eruption				
AV 7	Trapolino quarry. Top of the grey pumice fall deposit	0.70769 ± 1	—	—
AV 6	Trapolino quarry. Grey pumice fall deposit below AV7	0.70761 ± 1	0.70733 ± 1	0.70763 ± 1
AV 5s	Trapolino quarry. Hand split dark pumice below AV6 deposit	0.70760 ± 1	—	—
AV 5i	Trapolino quarry. Hand split intermediate pumice below AV6 deposit	0.70762 ± 2	—	—
AV 5c	Trapolino quarry. Hand split light pumice below AV6 deposit	0.70761 ± 1	—	—
AV 4	Trapolino quarry. Top of the white pumice fall deposit below AV5	0.70746 ± 1	—	—
AV 3	Trapolino quarry. White pumice fall below AV4	0.70729 ± 2	—	—
AV 2	Trapolino quarry. White pumice fall below AV3	0.70734 ± 2	0.70728 ± 1	0.70728 ± 1
AV 1	Trapolino quarry. Base of the white pumice fall	0.70742 ± 2	0.70729 ± 1	0.70743 ± 1
Pompei eruption				
84.41c	Pozzelle quarry. White pumice from the highest ash flow deposit	0.70761 ± 1	—	—
84.41s	Pozzelle quarry. Whitish pumice from the highest ash flow deposit	0.70759 ± 2	—	—
289	Pollena quarry. White pumice from ash flow 4	0.70767 ± 1	—	—
288	Pollena quarry. Grey pumice from ash flow 3	0.70750 ± 1	—	—
287	Pollena quarry. Grey pumice from ash flow 2	0.70749 ± 1	—	—
87.38	Pozzelle quarry. Grey pumice from the surge below the debris flow deposit	0.70749 ± 1	—	—
84.38	Same level as 87.38	0.70753 ± 1	—	—
87.37	Pozzelle quarry. Grey pumice from ash flow deposit below surge 87.38	0.70750 ± 1	—	—
84.37	Same level as 87.37	0.70754 ± 1	0.70778 ± 1	—
84.34	Pozzelle quarry. Grey pumice from the fallout deposit beginning the 3rd phase of the eruption (equivalent to sample 4 in Table 1)	0.70756 ± 2	—	—
87.33	Pozzelle quarry. Grey pumice from the pumice flow deposit closing the 2nd phase of the eruption	0.70754 ± 1	—	—
84.33	Same level as 87.33	0.70751 ± 1	—	—
294	Oplontis excavations. Top of the grey pumice fall deposit	0.70754 ± 1	—	—
158	Pompei excavations. Top of the grey pumice fall deposit	0.70752 ± 1	—	—
87.31B	Pozzelle quarry. Hand split darker pumice from the grey pumice fall deposit	0.70755 ± 1	—	—
87.31A	Pozzelle quarry. Same level as 87.31B: hand split lighter pumice	0.70752 ± 5	—	—
87.31	Pozzelle quarry. Same level as 87.31B, unsplit	0.70753 ± 1	0.70766 ± 1	—
293	Oplontis excavations. Grey pumice fall below 294	0.70754 ± 1	—	—
292	Oplontis excavations. Grey pumice fall below 293	0.70752 ± 1	—	—
291	Oplontis excavations. Grey pumice fall below 292	0.70751 ± 1	—	—
290B	Oplontis excavations. Base of the grey pumice fall	0.70751 ± 1	—	—
290A	Oplontis excavations. White pumice fall	0.70758 ± 1	—	—
84.30	Pozzelle quarry. Whitish pumice from the surge deposit topping the white pumice fall deposit	0.70760 ± 1	—	—
84.29	Pozzelle quarry. Top of the white pumice (equivalent to sample 6AV in Table 1)	0.70769 ± 2	0.70767 ± 1	—
87.28	Pozzelle quarry. White pumice fall below 84.29	0.70757 ± 1	—	—
157	Pompei excavations. White pumice fall deposit	0.70768 ± 1	—	—
87.27	Pozzelle quarry. White pumice fall below 87.28	0.70772 ± 1	—	—
84.26	Pozzelle quarry. Base of the white pumice fall (equivalent to sample 6V in Table 1)	0.70765 ± 1	0.70769 ± 1	—
87.26	Pozzelle quarry. White pumice from the ash fall of the very initial phase of the eruption	0.70778 ± 1	0.70779 ± 2	—
84.25	Same level as 87.26	0.70770 ± 2	—	—

Sample	Location	$^{87}\text{Sr}/^{86}\text{Sr}$ (whole rock)	Sr (ppm)
Carbonate xenolith 1	Pollena quarry	0.70765 ± 1	300
Carbonate xenolith 2	Pollena quarry	0.70772 ± 1	850
Carbonate xenolith 3	Pollena quarry	0.70775 ± 1	1000

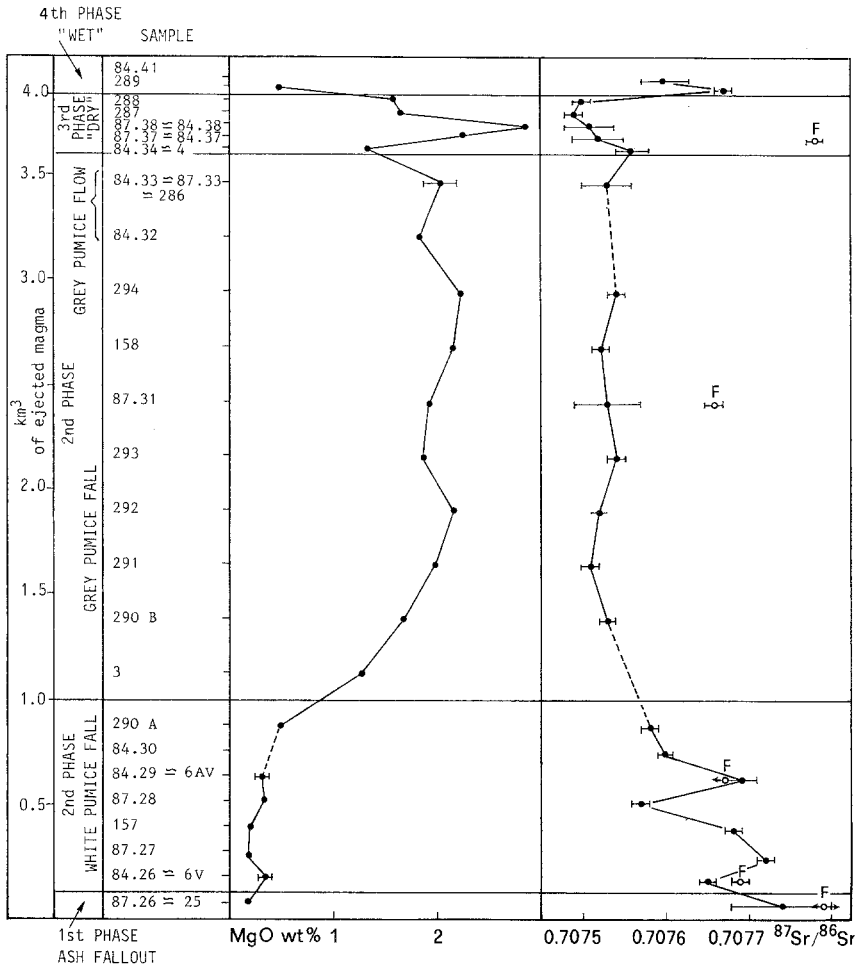
The average $^{87}\text{Sr}/^{86}\text{Sr}$ ratio of samples 84.41c and 84.41s, 288 and 287, 87.37 and 84.37, 87.33 and 84.33, 87.31A and 87.31B, 87.26 and 84.25 is reported in Fig. 6

and the $^{87}\text{Sr}/^{86}\text{Sr}$ ratio was measured on each duplicate sample. The difference is less than 0.03 per mil for all pairs, except for the basal one, where values of 0.70778 ± 1 and 0.70770 ± 2 were obtained. The $^{87}\text{Sr}/^{86}\text{Sr}$ ratio was also measured on eight K-feldspar separates (three from the Avellino sequence) and on three

separated glasses from Avellino samples. $^{143}\text{Nd}/^{144}\text{Nd}$ ratios were measured on eight samples, four of which were from the Avellino deposits. Results are listed in Table 5.

Table 5. $^{143}\text{Nd}/^{144}\text{Nd}$ ratio of composite pumice samples

Sample	Location	$^{143}\text{Nd}/^{144}\text{Nd}$
Avellino eruption		
AV 7	Trapolino. Upper grey pumice fall	0.512504 ± 6
AV 4	Trapolino. Upper white pumice fall	0.512524 ± 8
AV 2	Trapolino. Intermediate white pumice fall	0.512526 ± 7
AV 1	Trapolino. Lower white pumice fall	0.512526 ± 7
Pompei eruption		
84.41s	Pozzelle. Whitish pumice from the highest ash-flow deposit	0.512507 ± 10
289	Pollena. White pumice from ash flow 4	0.512476 ± 6
294	Oplontis. Top of the grey pumice fall	0.512507 ± 6
157	Pompei. White pumice fall	0.512496 ± 5

**Fig. 6.** Variations of $^{87}\text{Sr}/^{86}\text{Sr}$ ratio and $\text{MgO}\%$ of the pumice ejected during Pompei eruption. Within each phase of the eruption samples are arbitrarily spaced. Estimate of volume of the erupted magma (km^3 DRE) on the left. F = K-feldspar

Pompei pumice

The Sr isotopic ratio (whole rocks) depicts a trend roughly paralleling the observed chemical variations (Fig. 6). The white pumice exhibits a relatively wide range of $^{87}\text{Sr}/^{86}\text{Sr}$ ratios from 0.70778 to 0.70757. The range of the grey pumice is narrower (0.70756–0.70749). All the analysed K-feldspars have “white-pumice type” $^{87}\text{Sr}/^{86}\text{Sr}$ ratios (0.70766–0.70779), (Table 4 and Fig. 6). The $^{143}\text{Nd}/^{144}\text{Nd}$ ratio varies from 0.512476 to 0.512496 in white pumice. A slightly higher value (0.512507) was obtained for the grey pumice. All data plot in the “enriched” $^{87}\text{Sr}/^{86}\text{Sr}$ – $^{143}\text{Nd}/^{144}\text{Nd}$ quadrant (Fig. 8).

Avellino pumice

The Avellino isotopic pattern is exactly opposite to that of the Pompei pumice, with white pumice having an Sr-isotope composition constantly less radiogenic than the grey pumice (Fig. 7). The white pumice, as in Pompei, is characterized by higher variability of the $^{87}\text{Sr}/^{86}\text{Sr}$ ratio (0.70729–0.70746). The grey pumice exhibits a constant $^{87}\text{Sr}/^{86}\text{Sr}$ ratio (0.70761), with the exception of the top sample (AV7) showing the highest $^{87}\text{Sr}/^{86}\text{Sr}$ ratio recorded for the eruption (0.70769). Separated glass from samples AV1 (white) and AV6 (grey) is in isotopic equilibrium with the host whole pumice, but the glass

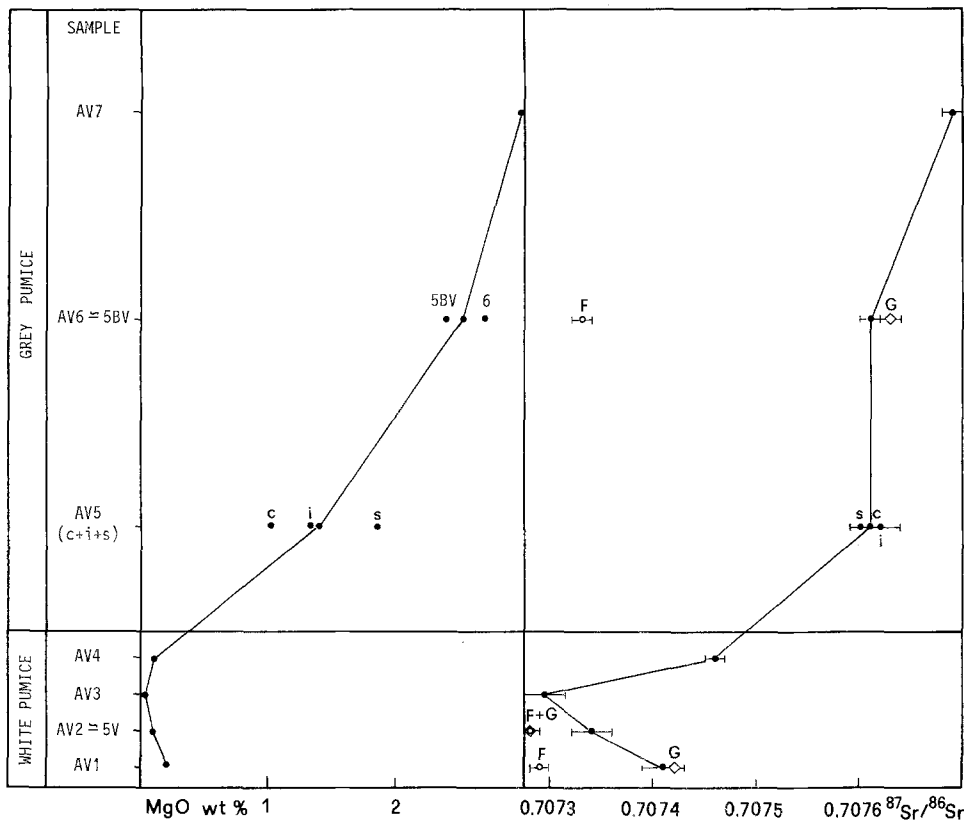


Fig. 7. Variations of $^{87}\text{Sr}/^{86}\text{Sr}$ ratio and MgO of the pumice ejected during the Plinian fallout phase of the Avellino eruption. The vertical scale represents the volume proportions of grey and white pumice, but no absolute values are provided because of the highly probable strong under-estimation of Lirer et al. (1973). Samples are arbitrarily vertically spaced. G, glass; F, K-feldspar

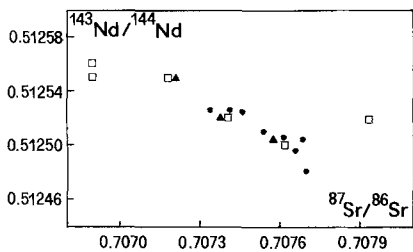


Fig. 8. $^{143}\text{Nd}/^{144}\text{Nd}$ vs $^{87}\text{Sr}/^{86}\text{Sr}$ plot of Somma-Vesuvius volcanic products. Full circle, Pompei and Avellino products; full triangle, Pollena products from Civetta et al. (1987); open square, Somma-Vesuvius products from Hawkesworth and Vollmer (1979), normalized to a BCR-1 value of 0.51266

of sample AV2 (white) is slightly less radiogenic than the whole pumice. As in Pompei, the K-feldspars have $^{87}\text{Sr}/^{86}\text{Sr}$ ratios (0.70728–0.70733) similar to that of the most evolved white pumice (AV3). $^{143}\text{Nd}/^{144}\text{Nd}$ ratios are higher (0.512524–0.512526) in the white pumice than in the grey one, (0.512504), here also reversing the Pompei trend. On the Nd vs Sr isotope diagram (Fig. 8) the Avellino pumice lies on the trend defined by the Pompei products.

Discussion

The absence of secondary minerals and the coherently inverse trend of Sr and Nd isotopic ratios rule out any significant role of post-eruptive alteration. The observed isotopic variation of Pompei and Avellino pu-

mice reflects, therefore, isotopic zoning in the magma chamber prior to eruption and discount closed-system fractional crystallization.

Isotopic variations within zoned magma chambers have been ascribed to: (1) radiogenic growth of ^{87}Sr within a long-lived magma chamber, zoned with respect to Rb/Sr (e.g. Mahood and Halliday 1988); (2) volatile phase transfer in a closed-system (Hildreth 1983); (3) crustal contamination (e.g. Wörner et al. 1985; Hildreth 1987); (4) magma mixing (e.g. Verma 1983).

The short life-time of the Vesuvius magmatic system and the low Rb/Sr exclude significant isotopic variations resulting from "in situ" radiogenic growth. Mass-dependent chemical fractionation of Sr and Nd, if present, cannot be detected because all data are normalized to constant $^{84}\text{Sr}/^{88}\text{Sr}$ and $^{146}\text{Nd}/^{144}\text{Nd}$ ratios; moreover a fluid preferentially enriched in ^{87}Sr isotope should provoke a radiogenic enrichment in the volatile-rich upper portion of the chamber and could not explain the contrasting isotopic patterns of the Avellino and Pompei sequences.

Evidence from xenolithic ejecta indicate the presence of a shallow magma chamber beneath Vesuvius. According to various geobarometric estimates (Barberi and Leoni 1980; Barberi et al. 1981; Belkin et al. 1985; Joron et al. 1987; Schoales et al. 1987), the top of this chamber is located within the Mesozoic calcareous sequence, at a depth ranging from 3 and 5 km. These rocks represent the most likely contaminant for both Pompei and Avellino magmas. $^{87}\text{Sr}/^{86}\text{Sr}$ and Sr content of carbonate xenoliths from Pompei deposits, range from 0.70765 to 0.70775 and from 300 to 1000 ppm (Ta-

ble 4). Cortini and Hermes (1981) reported a similar value (0.70768 ± 3) for a composite of carbonate ejecta collected from the Pompei products. $^{143}\text{Nd}/^{144}\text{Nd}$ of Jurassic carbonate rocks is today 0.51205 (Shaw and Wasserburg 1985).

Crustal assimilation, combined with fractional crystallization process (AFC; DePaolo 1981) could account for the isotopic variations recorded in both Avellino and Pompei sequences only by considering the lowest $^{87}\text{Sr}/^{86}\text{Sr}$ and the highest $^{143}\text{Nd}/^{144}\text{Nd}$ values as representative of uncontaminated (or less contaminated) magmas, and by assuming an increasing crustal contribution from grey to white pumice in Pompei, and from white to grey pumice in Avellino. This is shown in Fig. 9 where $^{87}\text{Sr}/^{86}\text{Sr}$ ratio is plotted versus Sr content. This figure reports the results of AFC modelling starting from the less-differentiated grey pumice (Pompei) and from the most-differentiated white pumice (Avellino), with a D_{sr} or 2.5 (Santacroce 1987) and with r (ratio between velocity of assimilation and velocity of crystallization) ranging from 0.5 to 0.9 (Pompei) and from 3 to 10 (Avellino). The ^{87}Sr and Sr richest xenolith is considered representative of the wall-rock contaminant material. This model requires different locations of the magma chamber (a possibility already suggested by Barberi et al. 1981), in such a way as to permit the maximum contamination effects to the lower "grey"

portion of Avellino magma and to the upper "white" portion of Pompei magma. Nevertheless, any modelling would result in contaminant/melt ratios close to or higher than one. This appears petrographically improbable, geochemically unbelievable and thermodynamically unrealistic.

The conclusion is that isotopically different magmas were involved in both Avellino and Pompei eruptions.

The occurrence of isotopic disequilibrium between sanidine and host pumice is evidence of syneruptive "white-grey" mingling. The separated sanidines from the Pompei pumice exhibit $^{87}\text{Sr}/^{86}\text{Sr}$ ratios revealing that they crystallized from "white melts". Mass balance calculations, using the sanidine content, indicate that between 5 and 20% of the grey magma was mingled with white magma. This would induce a moderate increase in the whole rock $^{87}\text{Sr}/^{86}\text{Sr}$ ratio, whose "original grey values" in the two calculated cases (samples 87.31 and 84.37 in Table 4) could be no higher than 0.70751 and 0.70746, respectively. The isotopic equilibrium between whole rock and sanidine in Pompei white pumice can be taken as an indication that the withdrawal from the magma chamber of the capping white pumice did not involve significant proportions of the grey component.

Avellino grey pumice (sample AV6, Table 4) also contains sanidine with a "white" $^{87}\text{Sr}/^{86}\text{Sr}$ ratio. Sanidine is on the liquidus of both grey and white Avellino pumice and, therefore, no simple calculations can be made to evaluate the syneruptive mingling. In contrast to Pompei, however, Avellino white pumice is not characterized by whole rock-sanidine isotopic equilibrium; sanidine is systematically less radiogenic than the host pumice (with the exception of the more evolved AV3 pumice, which probably represents the top layer within the chamber). This suggests that all through the Avellino eruption, magma ejection was accompanied by the mingling of the magma body between different layers.

A two end-member mixing between the two extreme compositions of the products of each eruption (Fig. 9) gives a reasonable explanation for the observed isotopic and geochemical variations. This model indicates that prior to the Avellino and Pompei eruptions (and probably prior to all the Plinian eruptions of Vesuvius; Civetta et al. 1987; R. Galati, unpublished data) the Vesuvius magma chamber was filled by an isotopically and compositionally homogeneous highly differentiated phonolitic magma (reference compositions could be samples 87.26 for Pompei and AV3 for Avellino). The arrival of a huge amount of geochemically and isotopically homogeneous mildly evolved magma, (reference samples 87.38 for Pompei and AV7 for Avellino) could have triggered the eruption with the consequent extrusion of variously mingled and mixed pumice fragments. A similar two end-member mixing model has been recently suggested by Sigurdsson et al. (1990) to explain the geochemical trends of the Pompei pumice.

This model, however, does not explain either the close geochemically affinity between the white and grey pumice of each deposit (clearly indicating fractional crystallization relation) or the compositional differ-

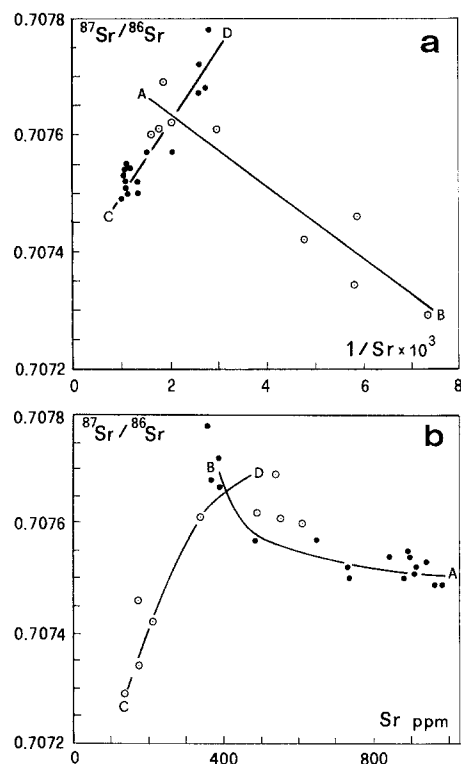


Fig. 9. a $^{87}\text{Sr}/^{86}\text{Sr}$ ratio vs $1/\text{Sr}$ of Pompei and Avellino pumice. Symbols as in Fig. 5. *AB* and *CD* represent mixing lines between the more and the less differentiated Pompei (*AB*) and Avellino (*CD*) pumice. b $^{87}\text{Sr}/^{86}\text{Sr}$ ratio vs Sr content of Pompei and Avellino pumice. Symbols as in Fig. 5. The *AB* (Pompei) and *CD* (Avellino) lines result by crystal fractionation combined with crustal assimilation process (AFC; DePaolo 1981). See text for discussion

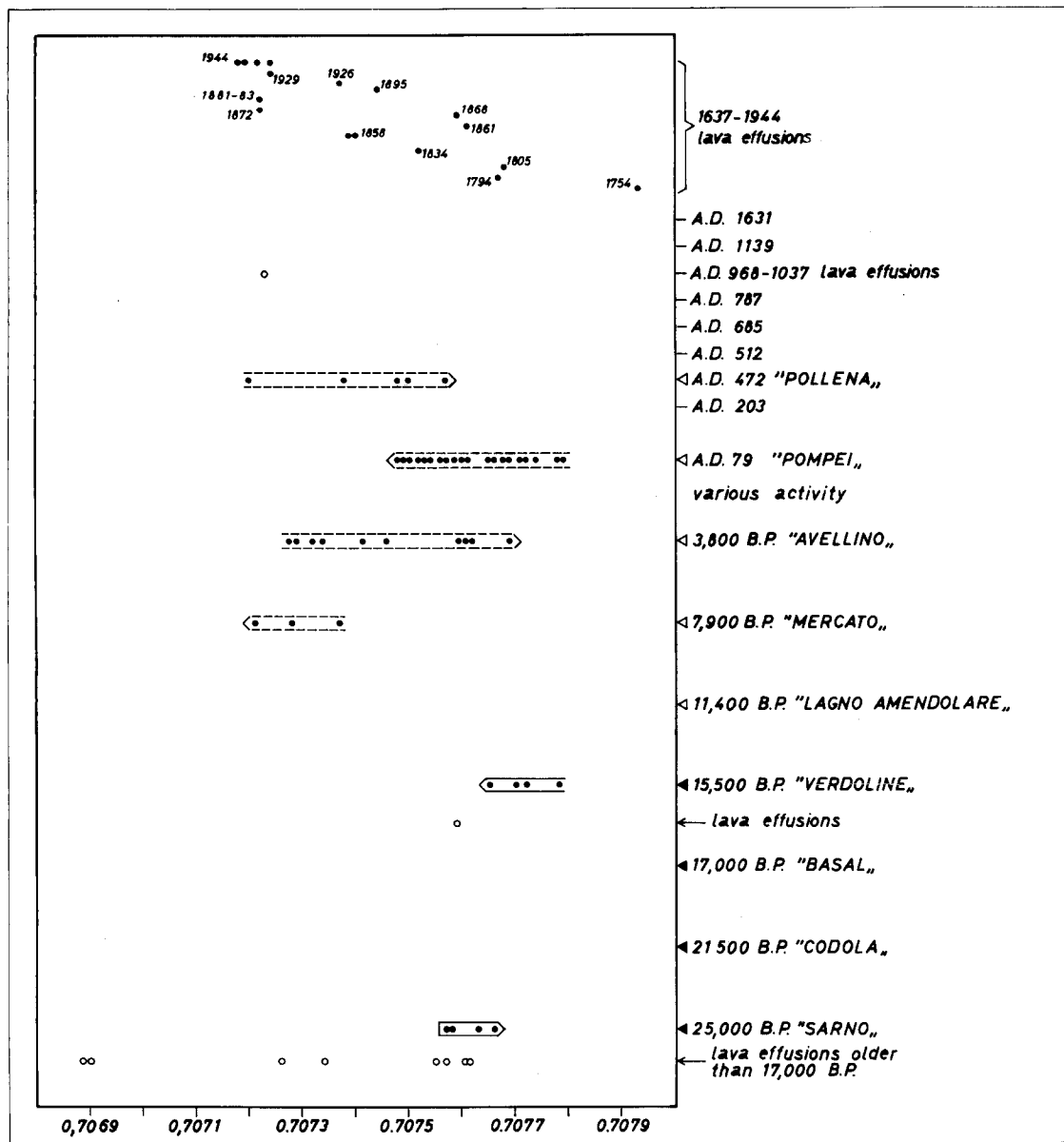


Fig. 10. $^{87}\text{Sr}/^{86}\text{Sr}$ ratio of Somma-Vesuvius volcanic products vs time of eruption (arbitrary scale). Data on lava samples are from Cortini and Hermes (1981); data on Sarno, Verdoline and Mercato Plinian eruptions are unpublished (L. Civetta and R. Galati); data on Pollena products are from Civetta et al. (1987). The value referred to 968–1037 lava effusions is sample PFSV 59 of Cortini

and Hermes (1981), erroneously ascribed to the 1631 eruption. The value referred to lava effusions between Basal and Verdoline Plinian eruptions is sample "B. di Pollena" from Cortini and Hermes (1981). Arrows indicate the variation from more evolved (generally first-erupted) to less-evolved products in zoned pyroclastic sequences of Plinian and subplinian eruptions

ences between the two sequences. Furthermore it remains necessary to explain why in both sequences the grey pumice has a fairly constant Sr-isotope composition, whereas the white pumice displays a range of $^{87}\text{Sr}/^{86}\text{Sr}$ ratios. As a matter of fact, the nearly homogeneous $^{87}\text{Sr}/^{86}\text{Sr}$ ratio of the Pompei grey pumice (0.70749–0.70756) suggests an isotopically well-mixed "grey layer" in the magma chamber. On the other hand, the variable $^{87}\text{Sr}/^{86}\text{Sr}$ of K-feldspar (0.70766–0.70779) and the whole rock (0.70757–0.70778) of the white pumice contrast the possibility of a single "white" convective layer. These data suggest the occurrence of a layered white portion of the magma body capping the

grey convective portion and cannot merely indicate syn-eruptive mingling.

The Avellino grey pumice (0.70760–0.70769) shows an homogeneous and high $^{87}\text{Sr}/^{86}\text{Sr}$ ratio, contrasting with the wider isotopic variability of the white pumice (0.70729–0.70746). The more pronounced chemical zonation of the Avellino grey pumice (Fig. 4) should reflect the waning convection within the isotopically homogeneous grey portion of the chambers and the establishment of a compositional gradient. We speculate that this can be the result of a slower recharge rate of the Avellino magma chamber in respect to the Pompei one.

In conclusion, the isotopic variations recorded in the deposits of the two eruptions do not result only by syneruptive mingling between two magmas, but probably reflect the more complex refilling history of the Vesuvius magma chamber.

According to Santacroce (1983), a key for understanding the Vesuvius behaviour is provided by the eruptive history of the 1637–1944 period of activity, characterized by open chimney conditions. In this period 18 short cycles of semi-persistent strombolian activity, separated by short quiescent periods, have been distinguished. Effusive eruptions were frequent within each cycle (“Intermediate Eruptions”), while more powerful explosive and lava eruptions (“Final Eruptions”) closed each cycle. It is thought that Final Eruptions emptied the plumbing system. Following short pauses of one to seven years, the system is refilled, thus the re-establishment of a near surface magma column is complete, and the resumption of strombolian activity starts a new cycle. The Intermediate Eruptions would reflect the periodic arrival of fresh magma batches in “full feeding system conditions” and consequent output of magma.

When the chimney is obstructed (preplinian conditions), the periodic deep magma supply will result in the shallow reservoir growing. Here magma experiences sidewall fractionation, reaction with country rocks and repeated mixing with newly arrived magma. The strong positive correlation between erupted volume, degree of evolution of the magma and repose time, characterizing the last 25 000 years of Somma-Vesuvius activity, is the basic element supporting the model of continuous refilling of the chamber (Santacroce 1983).

Isotopic data of other Vesuvius rocks agree with this model. As a matter of fact:

1. $^{87}\text{Sr}/^{86}\text{Sr}$ ratios measured on 13 lava samples of the recent activity (1754–1944; Cortini and Hermes 1981) emphasizes the different isotopic signature of each magma pulse. These data therefore allow a rather precise idea of the isotopic spectrum recorded during a refilling period several centuries long. The isotopic range (0.70718–0.70793) includes both Avellino and Pompei Sr-isotope ratios, and substantially repeats the isotopic variations recorded during the effusive activity older than 17 000 years (0.70689–0.70761, Cortini and Hermes 1981);
2. The $^{87}\text{Sr}/^{86}\text{Sr}$ variations recorded all along the time interval covered by samples analyzed by Cortini and Hermes (1981) are strongly “polarized”, with a progressive decrease from 0.7079 (1754 lava flow) to 0.7072 (1944 lava flow);
3. When $^{87}\text{Sr}/^{86}\text{Sr}$ ratios of pyroclasts from other Plinian and subplinian eruptions of Vesuvius are considered (Civetta et al. 1987; R. Galati, unpublished data), all exhibit significant chemical and isotopic variations. In each eruption the more evolved products are constantly the first to be ejected, while the isotopes show either an “Avellino pattern” (i.e. $^{87}\text{Sr}/^{86}\text{Sr}$ decreases with increasing differentiation) or a “Pompei pattern” (i.e. the $^{87}\text{Sr}/^{86}\text{Sr}$ increases with increasing differentia-

tion). If the Sr isotopic ratio of all Vesuvius products is plotted as a function of time (Fig. 10), it appears that, for adjacent events (no activity in between), the last-erupted, less-evolved magma of the older event has a $^{87}\text{Sr}/^{86}\text{Sr}$ ratio close to that of the first-erupted, more-evolved magma of the younger event.

Points 1 and 2 give a rather reliable idea of the isotopic spectrum expected during a refilling period, several centuries long, of the Vesuvius magma chamber. They suggest that such a refilling should occur through frequent and small magma pulses, each with a different isotopic ratio variable through time in a fairly regular way (either increasing or decreasing). As a rough order of magnitude, the eruptive record of the 1637–1944 period of activity of Vesuvius suggests at least 85 arrivals of new magma (mean frequency of magma arrival 15 each 3–4 years with a mean volume of $5\text{--}10 \times 10^6 \text{ m}^3$ each arrival) (data can be found in Santacroce 1987).

Conclusions

All the presented data and the previously discussed points (1, 2 and 3) suggest that the chemical and isotopic variations recorded in Avellino and Pompei deposits may be related to a repetitive history of magma refilling within the Vesuvius shallow reservoir. The process we suggest implies the existence of a “residual” magma chamber in which a significant amount of magma is left after the previous eruption. This magma, enriched in crystals and depleted in volatiles, is relatively basic in composition (tephritic-phonolitic in the Pompei and Avellino cases). New batches of magmas with different (increasing or decreasing through time) isotopic ratios enter the chamber. Each new magma batch will mix and convect with the less-differentiated deepest magma in the chamber. The mixed magma is subjected to magma chamber processes (sidewall crystallization, upward volatile concentration, etc.) and will tend to form a highly differentiated “white” portion capping the convective “grey” portion. In the first stages of the process the isotopic ratio of the white cap is strongly affected by the $^{87}\text{Sr}/^{86}\text{Sr}$ ratio of the magma left in the chamber after the preceding eruption. In the long run the new magma arrival will slightly change the isotopic ratio of the convective gray portion, progressively increasing the isotopic differences between the grey magma and the first generated white layer. The process will result in an increase over time of the white cap by repeatedly adjoining a new layer having the isotopic imprint of the last mixing episode. The less-differentiated white magma can either convectively mix or remain statically layered. In the first case, the system can be seen as a two-fold magma body, whose isotopic differences should progressively reduce over time and whose geochemical features of white and grey pumice should simulate quite well fractional crystallization, maintaining an abrupt compositional gap; in the second case a pronounced isotopic difference has to be expected within the white layered cap, and no clear relation of fractional-crystallization should characterize the less- and more-differentiated composition of the white

and grey pumice; in this case geochemical evidence of magma mixing is expected. The idea we have is that the concurrent effects of a relatively huge amount of the old residual magma and a relatively slow differentiation rate in producing white differentiated magma, could have the effect of "buffering" the process, enhancing the isotopic gap.

Acknowledgements. We are grateful to Steve Blake, Winton Cornell and Grant M. Heiken for their useful criticism. The research was sponsored by CNR (National Council of Research of Italy), Gruppo Nazionale per la Vulcanologia.

References

- Arnò V, Principe C, Rosi M, Santacroce R, Sbrana A, Sheridan MF (1987) Eruptive history, In Santacroce, R (ed), Somma-Vesuvius. CNR Quaderni de la ricerca scientifica, CNR, Roma 114:53-103
- Bacon CR, Druitt TH (1988) Compositional evolution of the zoned calcalkaline magma chamber of Mount Mazama, Crater Lake, Oregon. *Contrib Mineral Petrol* 98:224-256
- Barberi F, Innocenti F, Lirer L, Munno R, Pescatore T, Santacroce R (1978) The Campanian Ignimbrite: a major prehistoric eruption in the Neapolitan area (Italy). *Bull Volcanol* 41:1-22
- Barberi F, Bizouard H, Clocchiatti R, Metrich N, Santacroce R, Sbrana A (1981) The Somma-Vesuvius magma chamber: a petrological and volcanological approach. *Bull Volcanol* 44:295-315
- Barberi F, Leoni L (1980) Metamorphic carbonate ejecta from Vesuvius Plinian eruptions: evidence of the occurrence of shallow magma chamber. *Bull Volcanol* 43:107-120
- Barberi F, Cioni R, Rosi M, Santacroce R, Sbrana A, Vecchi R (1989) Magmatic and phreatomagmatic phases in explosive eruptions of Vesuvius as deduced by grain-size and compositional analysis of pyroclastic deposits. *J Volcanol Geothermal Res* 38:287-307
- Barberi F, Navarro JM, Rosi M, Santacroce R, Sbrana A (1990) Explosive interaction of magma with ground water: insights from xenoliths and geothermal drillings. *Rend Soc Ital Mineral Petrol Spec Iss* (in press)
- Belkin HE, De Vivo B, Roedder E, Cortini M (1985) Fluid inclusion geobarometry from ejected Mt. Somma-Vesuvius nodules. *Amer Mineral* 70:288-303
- Carey S, Sigurdsson H (1987) Temporal variations in column height and magma discharge rate during the 79 A.D. eruption of Vesuvius. *Geol Soc Am Bull* 99:303-314
- Civetta L, D'Antonio M, Paone E, Santacroce R (1987) Isotopic studies of the products of the 472 Pollena eruptions (Somma-Vesuvius). *Boll GNV*:263-271
- Cornell W, Sigurdsson H (1984) Modeling of trace element gradients in the Vesuvius 79 A.D. reservoir. *Eos*:65, 1128
- Cornell W, Sigurdsson H (1987) Compositional zoning in the Pompei 79 A.D. pumice deposit: magma mixing and observed trends. *Eos*:68, 434
- Cortini M, Hermes OD (1981) Sr isotopic evidence for a multi source origin of the potassic magmas in the Neapolitan area. *Contrib Mineral Petrol* 77:47-55
- Delibrias G, Di Paolo GM, Rosi M, Santacroce R (1979) La storia vulcanica del complesso vulcanico ricostruita dalle successioni piroclastiche del Monte Somma. *Rend Soc It Mineral Petrol* 35:411-438
- DePaolo DJ (1981) Trace elements and isotope effects of combined wall-rock assimilation and fractional crystallization. *Earth Planet Sci Lett* 53:189-202
- Fridrich CJ, Mahood GA (1987) Compositional layers in the zoned magma chamber of the Grizzly Peak Tuff. *Geology* 15:299-300
- Hawkesworth CJ, Vollmer R (1979) Crustal contamination versus enriched mantle. $^{143}\text{Nd}/^{144}\text{Nd}$ and $^{87}\text{Sr}/^{86}\text{Sr}$ evidence from the Italian volcanics. *Contrib Mineral Petrol* 69:151-165
- Hildreth W (1979) The Bishop Tuff: evidence for the origin of compositional zonation in silicic magma chambers. *Geol Soc Am Spec Pap* 180:43-75
- Hildreth W (1981) Gradients in silicic magma chambers: Implication for lithospheric magmatism. *J Geophys Res* 86:10153-10192
- Hildreth W (1983) Chemical differentiation of the Bishop Tuff and other high-silica magmas through crystallization processes: comments. *Geology* 11:622-623
- Hildreth W (1987) New perspectives on the eruption of 1912 in the Valley of Ten Thousand Smokes, Katmai National Park, Alaska. *Bull Volcanol* 49:680-693
- Joron JL, Metrich N, Rosi M, Santacroce R, Sbrana A (1987) Chemistry and petrography, In Santacroce, R (ed) Somma-Vesuvius. *Quaderni de la ricerca scientifica, CNR, Roma* 8:105-171
- Lirer L, Pescatore T, Booth B, Walker GPL (1973) Two Plinian pumice-fall deposits from Somma-Vesuvius, Italy. *Geol Soc Am Bull* 84:759-772
- Macedonio G, Pareschi MT, Santacroce R (1989) A numerical simulation of the Plinian fall phase of 79 A.D. eruption of Vesuvius. *J Geoph Res* 93: B 12:14817-14827
- Mahood GA, Halliday AN (1988) Generation of high-silica rhyolite: A Nd, Sr and O isotopic study of Sierra La Primavera, Mexican Neovolcanic Belt. *Contrib Mineral Petrol* 100:183-191
- Palacz ZA, Wolff JA (1989) Strontium, Neodinium and lead isotopes characteristics of the Granadilla pumice, Tenerife: a study of the causes of strontium isotope disequilibrium in felsic pyroclastic deposits. In: AD Saunders, MJ Norry (eds) *Magmatism of ocean basin*. *Geol Soc Spec Publ* 42
- Santacroce R (1983) A general model for the behaviour of the Somma-Vesuvius volcanic complex. *J Volcanol Geoth Res* 17:273-248
- Santacroce R (ed) (1987) *Somma-Vesuvius. Quaderni de la Ricerca Scientifica, CNR, Roma* 114:1-251
- Schoales DY, Rutherford NJ, Sigurdsson H (1987) Conditions in the magma chamber prior to the 79 A.D. eruption of Mt Somma-Vesuvius. *EOS* 68:434
- Shaw HF, Wasserburg GI (1985) Sr-Nd in marine carbonates and phosphates. Implications for Nd isotopes in seawater and crustal ages. *Geoch Cosmoch Acta* 49:503-518
- Sheridan MF, Barberi F, Rosi M, Santacroce R (1981) A model for Plinian eruptions of Vesuvius. *Nature* 289:282-285
- Sigurdsson H, Carey S, Cornell W, Pescatore T (1985) The eruption of Vesuvius in 79 A.D. *National Geographic Res* 1:332-387
- Sigurdsson H, Cashdollar S, Sparks RSJ (1982) The eruption of Vesuvius in A.D. 79: Reconstruction from historical and volcanological evidence. *Am J Archaeol* 86:39-51
- Sigurdsson H, Cornell W, Carey S (1987) Dynamics of magma withdrawal during the 79 A.D. eruption of Vesuvius. *EOS* 68, 16:434
- Sigurdsson H, Cornell W, Carey S (1990) Influence of magma withdrawal on compositional gradients during the AD 79 Vesuvius eruption. *Nature* 345:519-521
- Spera FJ, Yuen DA, Greer JC, Sewell G (1986) Dynamics of magma withdrawal from stratified magma chambers. *Geology* 14:723-726
- Turner JS (1980) A fluid-dynamical model of differentiation and layering in magma chambers. *Nature* 285:213-215
- Verma SP (1983) Magma genesis and chamber processes at Los Hornos caldera, Mexico - Nd and Sr isotope data. *Nature* 302:52-55
- Wolff JA, Storey M (1984) Zoning in highly alkaline magma bodies. *Geol Mag* 121:563-575
- Wörner G, Staudigel H, Zindler A (1985) Isotopic constraints on open system evolution of the Laacher See magma chamber (Eifel - West Germany) *Earth Planet Sci Lett* 75:37-44